Quaternary Science Reviews 30 (2011) 1185–1200

Contents lists available at ScienceDirect

Quaternary Science Reviews

journal homepage: www.elsevier.com/locate/quascirev

Chronology of the Lower–Middle Pleistocene succession of the south-western part of the Crotone Basin (Calabria, Southern Italy)

L. Capraro [a,*], F. Massari [a], D. Rio [a], E. Fornaciari [a], J. Backman [b], J.E.T. Channell [c], P. Macrì [d,e], G. Prosser [e], F. Speranza [d]

[a] Department of Geosciences, Via Gradenigo 6, I-35100 Padova, Italy
[b] Department of Geology and Geochemistry, S-10691 Stockholm, Sweden
[c] Department of Geological Sciences, POB 112120, Gainesville, FL-32611, USA
[d] Istituto Nazionale di Geofisica e Vulcanologia, Via di Vigna Murata, 605, I-00143 Rome, Italy
[e] Department of Geological Sciences, Campus Macchiaromana I-85100 Potenza, Italy

ARTICLE INFO

Article history:
Received 13 May 2010
Received in revised form
15 February 2011
Accepted 17 February 2011
Available online 25 March 2011

Keywords:
Pleistocene
Chronostratigraphy
Southern Italy

ABSTRACT

Biostratigraphy based on calcareous nannofossils, integrated by magnetostratigraphic, geochronological and isotopic data, allowed establishing a precise chronological framework for the Pleistocene succession within the south-western sector of the Crotone Basin (Calabria, Southern Italy), where the Pliocene–Pleistocene global stratotype section and point is defined, thus demonstrating that sedimentation was quasi-continuous during most of the Lower and Middle Pleistocene.

At a large scale, the Pleistocene succession in this sector of the Crotone Basin is characterized by an evident shallowing-upwards trend, showing facies changes from bathyal to shelfal to littoral/continental. However, comparison between adjacent sectors within the investigated area demonstrates that stratigraphic architectures change vastly on very short distances. Our chronological constraints indicate that such changes in sedimentation styles probably occurred in response to differential subsidence rates, which originated tectonically-controlled synsedimentary structures where accommodation space and sediment yield were allotted unevenly. This articulated physiography led to striking differences in the overall thicknesses and organization of Pleistocene stratigraphies and, eventually, to a distinct diachroneity in the first appearance of shallow-marine deposits. In addition, superimposed are complex interplays between regional and local tectonics, eustasy and orbitally-forced climate changes. These interactions have been highlighted by the oxygen isotope stratigraphy established for a part of the studied succession, which is likely to document almost continuously the interval from Marine Isotope Stage (MIS) 26 to MIS 17. In its younger part (post-MIS 17), chronological ties are poor, as the succession is dominated by shallow-water to continental deposits showing a prominent organization into cyclothems. Nevertheless, based on the chronology of the underlying units, it is feasible that basin infill ended during MIS 15-MIS 14 times.

© 2011 Elsevier Ltd. All rights reserved.

1. Introduction

Thick Lower and Middle Pleistocene successions were laid down with exceptionally high sedimentation rates in the Crotone Basin (Calabrian arc: Fig. 1) which was uplifted in very recent times, as evidenced by a flight of Pleistocene marine terraces which can be followed along the entire Ionian margin.

The availability of extensive outcrops of slope to shelf mudstones, which hold remarkable stratigraphic continuity and high sensitivity to environmental changes, provides the rare opportunity of studying in high resolution an expanded marine record of the Pleistocene. In particular, hemipelagic facies represent an important part of the succession, thus permitting the employment of conventional biostratigraphic and magnetostratigraphic tools along with stable oxygen isotopes analyses. In previous investigations (Rio et al., 1996; Massari et al., 2002; Capraro et al., 2005) a solid time framework was established for the Lower and Middle Pleistocene successions in the northern part of the onshore Crotone Basin (particularly in the San Mauro area). An integrated approach emphasized the presence of a pervasive cyclicity, which can be defined in terms of both frequency and amplitude, and correlated with the astronomically-forced climatic variability (Capraro et al., 2005; Massari et al., 2007).

* Corresponding author.
E-mail address: luca.capraro@unipd.it (L. Capraro).

0277-3791/$ – see front matter © 2011 Elsevier Ltd. All rights reserved.
doi:10.1016/j.quascirev.2011.02.008

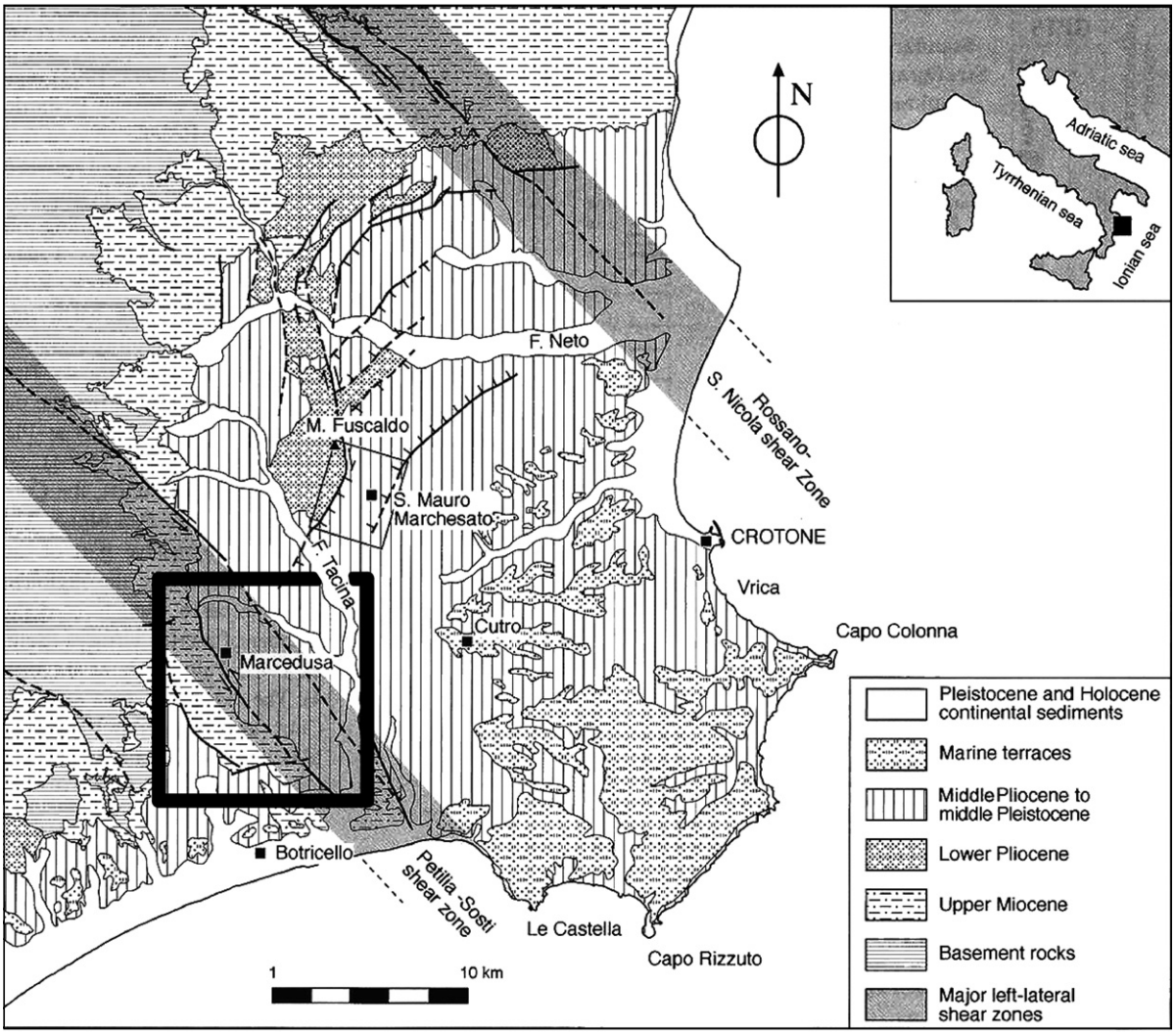

Fig. 1. Tectonic sketch-map of the onshore Crotone Basin. Box shows the location of the geological map of Fig. 2.

Here we present and discuss a new dataset concerning the chronology of the Pleistocene succession in the south-western part of the Crotone Basin (Fig. 2). These data provide a substantial update of the chronological framework available so far, which is of the essence for constraining in time the beginning of regional uplift and, eventually, the molding of marine terraces during the latest Middle and Late Pleistocene.

2. Geologic setting

The late Neogene to Quaternary Crotone Basin is a forearc basin located above the internal part of the Calabrian accretionary wedge (Rossi and Sartori, 1981; Barone et al., 1982; Van Dijk, 1991) and houses one of the thickest (more than 3000 m) and best-exposed sedimentary successions of Southern Italy (Fig. 1). Its late Neogene evolution is closely linked to the tectonic history of the Apennnic–Maghrebid thrust belt and to the rapid opening of back-arc basins in the Tyrrhenian Sea, in the wake of the outward migrating Calabrian Arc.

It is generally admitted that the migration of the Calabrian Arc occurred in a framework of a progressive retreating, old and dense oceanic Ionian lithosphere (Ritsema, 1979; Malinverno and Ryan, 1986; Sartori, 2003). Rate of subduction exceeded the rate of convergence, implying regional extension in the upper plate, and specifically a long-living extensional regime in the Crotone forearc basin. This regime, active since the late Miocene, was however punctuated by apparently brief transpressional episodes, in the late Messinian, the late Early Pliocene and possibly also the late Early Pleistocene (Roda, 1964; Van Dijk, 1992).

After the contractional episode of the late Early Pliocene, a long-lasting extensional sedimentary-tectonic regime was established in the Crotone Basin during the Middle and Late Pliocene and Early Pleistocene, accompanied by high subsidence rates, as documented by the accumulation of an exceptionally thick succession of dominantly slope mudstones (Fig. 2) (Ogniben, 1955; Roda, 1964; Van Dijk, 1992). This regime led to a profound reorganization of the paleogeography, with generalized transgression and stratigraphic onlaps, and was characterized by rapid south-eastward migration of the Calabrian Arc, and very fast opening of the Marsili Basin in the back-arc area (Rossi and Sartori, 1981; Sartori, 1990; Van Dijk and Okkes, 1991; Patacca et al., 1993).

A major tectonic reorganization in the whole central Mediterranean area is currently believed to have taken place during the Middle Pleistocene (Anderson and Jackson, 1987; Lucente et al., 1999; Patacca and Scandone, 2004; Goes et al., 2004; Jenny et al., 2006), and regarded as the effect of docking of Calabria between

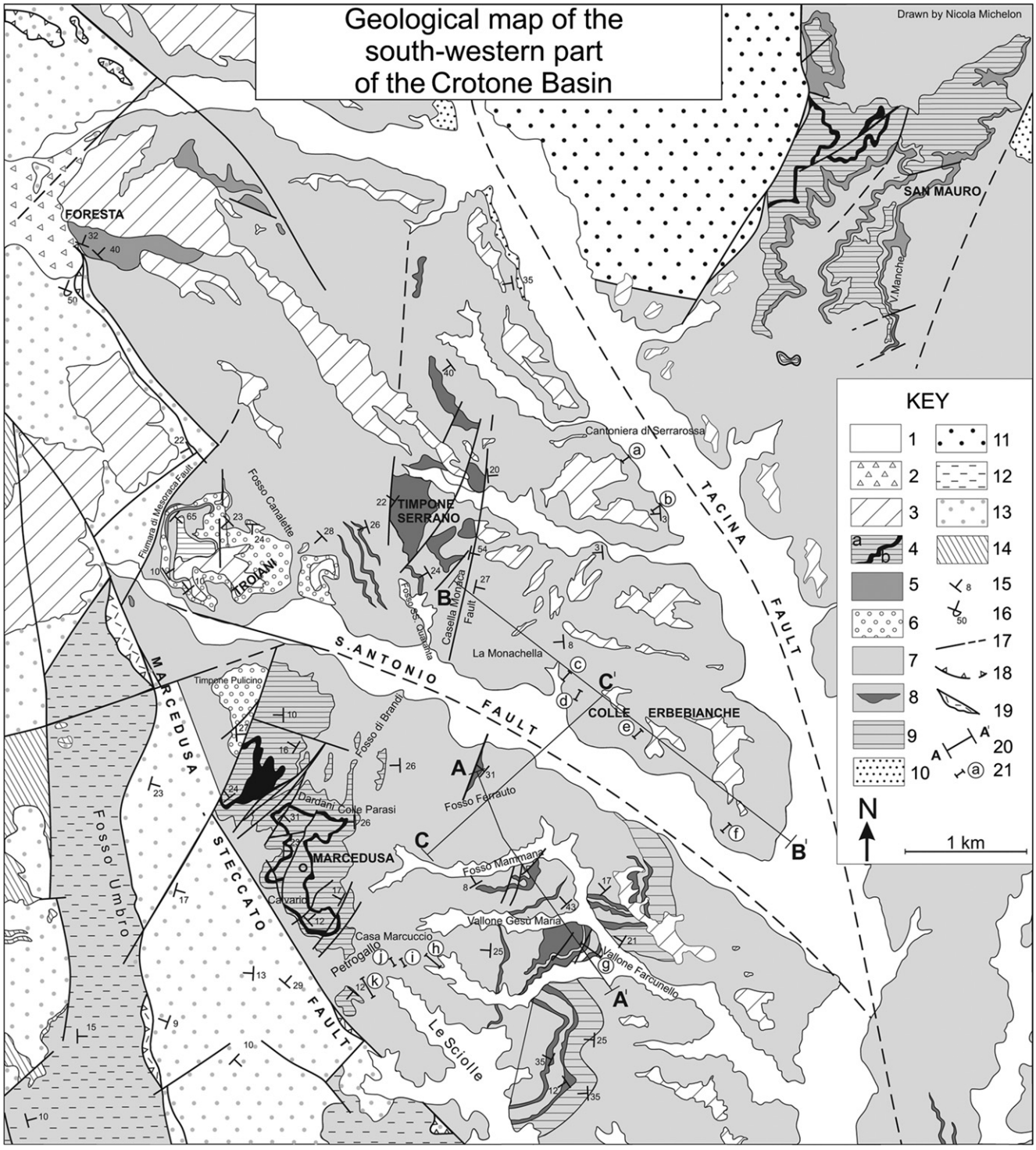

Fig. 2. Simplified geological map of the southern part of the onshore Crotone Basin. 1: Recent fluvial deposits; 2: Talus deposits (Pleistocene–Holocene); 3: Gravels and sands of fluvial terraces and pediment cover (Middle–Upper Pleistocene); 4: Sand-dominated transgressive–regressive cyclothems of the younger part of the Crotone Basin fill (a), and mappable transgressive horizons (b) (MIS 18-?MIS 8); 5: Progradational shoreface body consisting of mixed bioclastic–siliciclastic arenite/rudite (dated to MIS 24-22 in San Mauro area:); 6: Delta-front sandstones (Troiani area: ?MIS 24-22); 7: Slope hemipelagic marls to mudstones, with local thin-bedded turbidites, passing to outer-shelf mudstones in the upper part of the succession [Cutro Marly Clay (Roda, 1964): Uppermost Zanclean to Middle Pleistocene, developing up to MIS 19 in the San Mauro area and up to ?MIS 10 in the Marcedusa area]; 8: Turbiditic sandstone bodies within Cutro Marly Clay (uppermost Gelasian and Lower Pleistocene); 9: Diatomaceous laminated horizons interbedded with hemipelagic mud, commonly grouped into clusters (Gelasian); 10: Sandstone-dominated shallow-marine fossiliferous cyclothems (Scandale Sandstone: ?Middle Pliocene); 11: Fossiliferous shoreface sandstone (Zinga Sandstone: ?Zanclean); 12: Marls locally grading upwards into a flysch-like facies with thin-bedded turbidites (Cavalieri Marl: Zanclean); 13: Undifferentiated pre-Pliocene (upper Serravallian (?) to Messinian) deposits; 14: Paleozoic basement; 15: Normal bed attitude; 16: Reversed bed attitude; 17: Fault; 18: Reverse fault; 19: Tectonic breccia and megabreccia with chaotic fabric, mostly consisting of randomly oriented Messinian fragments and olistoliths in a fine-grained matrix, forming lenticular bodies along reverse faults; 20: AA′, BB′, CC′: traces of measured sections; 21: Measured sections. a: Case Tufilica; b: Destra Tacina; c: La Celsa N; d: La Celsa NE; e: Cantoniera Erbebianche; f: Timpone Giordano; g: Timpone Baronello; h: Lamalunga; i: Marcuccio E; j: Marcuccio W; k: Petrogallo.

Apulia and Sicily, resulting in stop or significant slowing down of the Calabrian Arc subduction and accompanying Tyrrhenian back-arc extension, as well as onset of uplift of the Calabrian block.

Although regional analysis of the relief indicates that the regional Quaternary uplift has a complicated interaction with the rates of local active faulting (Molin et al., 2004), the marine terraces of the coastal belt of Calabria record an average uplift rate of 0.6–1.0 mm/yr (Lanzafame and Tortorici, 1981; Carobene and Dai Pra, 1990; Tortorici et al., 1995; Mauz and Hassler, 2000; Nalin et al., 2007). The average uplift rate agrees with that reported at a regional scale for the southern Apennines (Westaway, 1993; Schiattarella et al., 2006).

The investigated area is located in the south-western part of the onshore Crotone Basin (Figs. 1 and 2). Fig. 2 shows the position of the logged key Segments and reference to the areas where main parts of the succession crop out.

3. Material and methods

Because of the overall monotonous lithology in the open-marine mud-dominated parts of the succession, intrabasinal correlations based on physical evidence are often difficult. This complication has been (partly) untangled by achieving a high-resolution chronologic framing of the succession, based on correlation between field evidences and bio-magnetostratigraphic data. Several sections were logged and sampled with variable sampling resolutions, eventually resulting in the collection of an estimated amount of more than 700 samples (preliminary test samples included). Weight of the standard hand-picked bulk samples varied from ca 100–200 g, which was largely sufficient for all routine analyses; smaller (toothpick) samples were collected for very preliminary test investigations. From the bulk samples, fragments of ca 50 and 20 g were isolated to be prepared for foraminiferal and pollen analyses, respectively. Results are not presented here and will be discussed in a forthcoming paper. For nannofossil biostratigraphic analyses, a small sediment shard was processed according to standard methods for smearslides, which were examined using a light microscope at 125× magnification. Investigation was performed following either quantitative or semiquantitive methods, namely: (a) for the Petrogallo composite section, counting of at least 500 nannofossil specimens (Thierstein et al., 1977), or (b) counting of a prefixed number of taxonomically related forms (i.e., 30–50 *Helicoliths* and 10–30 *Calcidiscus*: Rio et al., 1990), or (c) counting of the number of specimens from selected species in a smear-slide area of ca 1 mm^2 (Backman and Shackleton, 1983). For biostratigraphic purposes, we employed the zonation of Rio et al. (1990); biochronology was based on the astrocyclostratigraphically-calibrated ages of Castradori (1993), Raffi et al. (1993), Lourens et al. (1996) and Lourens (2004) (Fig. 3). A number of spots were selected for attaining magnetostratigraphic information. Samples for paleomagnetic analysis were either hand-picked or drilled using a petrol-powered portable drill, and oriented before extraction by a magnetic compass corrected to account for the current mean magnetic declination of the local geomagnetic field (ca +2° according to Istituto Nazionale di Geofisica e Vulcanologia, 2007). Measurements were performed at the paleomagnetic laboratories of the Department of Geology of the University of Florida (for the Petrogallo Composite and the Marcuccio E sections) and of the INGV of Rome (for the others). Characteristic remnant magnetization directions (ChRMs) were isolated by means of a progressive thermal demagnetization; data were plotted according to Zijderveld (1967) (Fig. 4) and the magnetization components were isolated by principal component analysis (Kirschvink, 1980). As a rule, a viscous component was eliminated at 180–220 °C and a ChRM was isolated in the 180°–220° to 380°–460 °C temperature interval. In most of the studied sections, the individual ChRMs define a succession of normal- and reverse-polarity magnetozones.

Stable oxygen isotope stratigraphies were obtained in the key Valle di Manche and Petrogallo sections, located near the villages of San Mauro and Marcedusa, respectively (Fig. 2). After washing the sample with deionized water and sieving of the coarse fraction at 63 μm, hand-picked foraminifer specimens showing no traces of diagenetic alteration were selected under an optical stereomicroscope, ultrasonically cleaned in order to remove contaminants (coccoliths, overgrowths and detrital infilling) and roasted under vacuum at about 350 °C for 2 h. Analyses were performed by a Finnigan MAT 252 mass spectrometer at the Department of Geology and Geochemistry of the Stockholm University. Results are presented as per mil (‰) deviation with respect to the PDB standard. The reproducibility of the measurements is ±0.1‰. In these sections, a quasi-continuous oxygen isotope stratigraphy has been established for the benthic foraminifer *Uvigerina peregrina* and, where available, for the planktonic foraminifer *Globigerinoides ruber*.

Biostratigraphic and magnetostratigraphic data of individual logs is reported in Fig. 5a and b.

4. Chronology

The stratigraphic succession exposed in the studied area can be subdivided into two main units: a lower (older) unit, generally characterized by deep, open-marine sedimentation, and an upper (younger) unit, which in turn documents the gradual shallowing of the basin and its emergence. However, establishing a detailed age model is not straightforward and chronology of the younger part of the stratigraphy is still controversial, as discussed below.

4.1. The lower part of the succession

In the investigated area, a Lower Pleistocene stratigraphy (up to the "large" *Gephyrocapsa* Zone included) is widely exposed that is generally represented by slope deposits. However, logged sections commonly display significant differences in terms of sedimentation rates and style, yet at a short distance. This feature is especially impressive when comparing the stratigraphies exposed on either sides of the San Antonio River (Fig. 2), which are dramatically different in spite of their fully comparable ages (Fig. 6). Based on the distribution of peculiar sedimentary features, as described below, we identified three sectors, boundaries of which are unfortunately not exposed, showing a distinct internal homogeneity in their stratigraphic organization. Sectors have been subdivided as follows (Fig. 7):

1) In Sector 1 (south of the San Antonio River: sections *g* to *k* in Fig. 2), the succession spanning the *C. macintyrei*, *H. sellii*, and "large" *Gephyrocapsa* Zones (around 450 m thick, 360 m from the base of the *H. sellii* Zone) is characterized by the presence of recurrent laminated sapropel-like layers; interbedded with massive slope mudstones are three major lenticular, turbidite-bearing sandstone bodies, showing limited lateral persistence (Figs. 6 and 7). The latter are best exposed in the Timpone Baronello section, where the Pliocene–Pleistocene (Gelasian–Calabrian) boundary has been identified (Fig. 5a). Fig. 8 shows the biostratigraphy of the Lower Pleistocene succession across two exemplary transects within this Sector.
2) In Sector 2 (Timpone Serrano area, north-west of the San Antonio River), stratigraphic organization of the Lower Pleistocene succession is comparable to that of the Marcedusa sector, showing a number of lenticular sandstone bodies encased within slope mudstones (Fig. 7). However, the overall succession (about 200 m from the base of the *H. sellii* Zone to the top of the "large" *Gephyrocapsa* zone) and individual

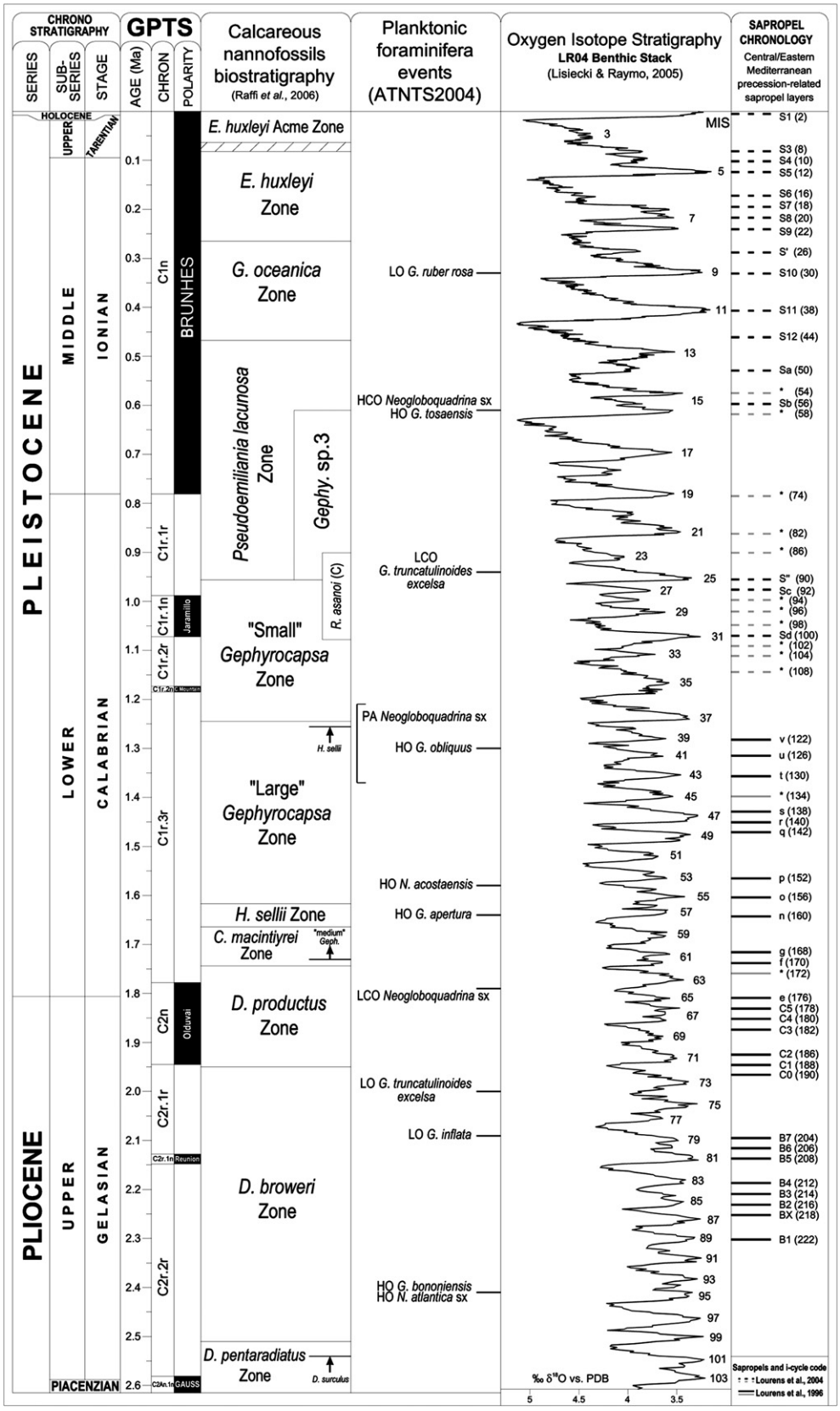

Fig. 3. Adopted time framework. Geomagnetic Polarity Time Scale (GPTS) after Lourens et al. (1996). Calcareous nannofossils biostratigraphy after Raffi et al. (2006). Planktonic foraminifera events after Lourens (2004). Standard oxygen isotope stratigraphy after Lisiecki and Raymo (2005). Mediterranean sapropel layers after Lourens et al. (1996) and Lourens (2004).

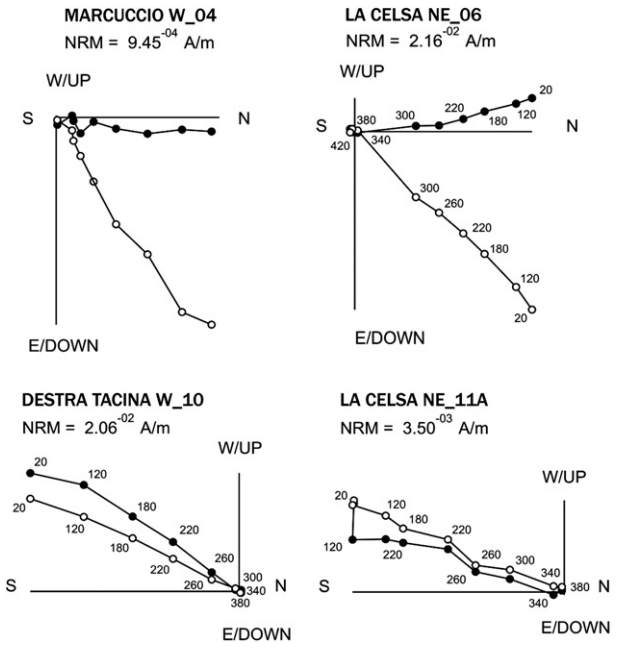

Fig. 4. Exemplary orthogonal vector diagrams of typical thermal demagnetization data, tilt-corrected coordinates. Open (solid) circles represent projections on the vertical (horizontal) plane.

sandstone bodies are significantly thinner. In addition, no sapropel-like layers have been identified in this sector.

3) In Sector 3 (Colle Erbebianche area, north-east of the San Antonio River: sections *a* to *f* in Fig. 2), the Lower Pleistocene stratigraphy is strikingly different in terms of facies and sedimentation style from that of the adjacent areas, as it consists exclusively of hemipelagic muds almost devoid of sapropel-like layers and completely devoid of sand bodies (Figs. 6 and 7). Here, the overall thickness of the interval encompassing the *C. macintyrei* to "large" *Gephyrocapsa* Zones is around 110 m (75 m from the base of the *H. sellii* Zone), thus indicating a significantly lower average sedimentation rate if compared with the adjacent areas.

Since a logical succession of nannofossil biohorizons can be predictably traced from Sector 1 to Sector 3 (Fig. 7), we infer that differential subsidence rates may have played a key role by leading to the growth of syndepositional highs and lows. In the light of available data, it can be assumed that during Early Pleistocene times a major structural divide developed grossly in correspondence to the present San Antonio river valley (namely, the San Antonio Divide, SAD for brevity). Specifically, Sectors 1 and 2 may be regarded as branches of a depositional trough generally affected by high subsidence rates and therefore capable of large sediment storage (Figs. 5a,b and 7); nonetheless, Sector 2 developed lesser accommodation space, possibly in response to synsedimentary activity of the Casella Monaca Fault (Fig. 7).

In turn, the stratigraphic record of Sector 3 is consistent with a setting of structural/physiographic high, subject to lower subsidence rates than the adjacent sectors and probably prone to sediment bypass.

4.2. The upper part of the succession

In the investigated area, age of the younger part of the stratigraphy is late Early to Middle Pleistocene. Distinctive trait of this part of the succession is the rapid, yet generally gradual, transition from outer shelf/slope mudstones to middle/inner-shelf cyclothems and, eventually, to marginal-marine and continental deposits. Deposits of this age are confined within four areas, namely the San Mauro, Foresta, Troiani and Marcedusa areas (Fig. 2), which host distinct stratigraphic successions, mostly in terms of the age of the first appearance of shallow-water units. Specifically, in the San Mauro, Foresta and Troiani areas the shallow-water facies appeared much earlier (Early Pleistocene biocalcarenite and sandstone, correlated in the San Mauro area with the glacial MIS 24-22 by Rio et al., 1996) than in the Marcedusa area (late Middle Pleistocene).

4.2.1. The San Mauro area

We are not providing here new data, as the stratigraphic succession cropping out in this key area was extensively studied and described (physical stratigraphy, chronology, pollen, stable oxygen isotopes) by previous investigations (Rio et al., 1996; Massari et al., 1999; Massari et al., 2002; Capraro et al., 2005; Massari et al., 2007). The San Mauro succession displays an overall regressive trend from slope/shelf mudstones to shallow-water to marginal-marine/continental cyclothems (Fig. 9). A major erosional unconformity is documented, whose gap suppresses the upper part of the "large" *Gephyrocapsa* Zone (locally the entire "large" *Gephyrocapsa* Zone) and the lower part of the "small" *Gephyrocapsa* Zone. The succession is interpreted to span up to ?MIS 9-8 (ca 0.3 Ma, *G. oceanica* Zone).

4.2.2. The Foresta area

The local succession (Fig. 9) consists of ca 65 m of upward shallowing outer- to inner-shelf, highly fossiliferous silty mudstones, straddling the boundary between the "large" *Gephyrocapsa* and the "small" *Gephyrocapsa* Zones, overlain by a package ca 35 m thick of innermost shelf to lower shoreface deposits, consisting of fine sands and coarse bioclastic calcarenites unsuitable to biostratigraphic analyses.

4.2.3. The Troiani area

In this area (Fig. 9), the Lowest Occurrence (LO) of *Gephyrocapsa* sp.3 (=MIS 25) has been documented in mudstones that are overlain by a mixed biocalcarenite/sandstone shallow-water unit, interpreted as the record of delta-front to shoreface settings. The younger deposits of the Troiani sector are represented by a shallow-water transgressive–regressive cyclothem which is tentatively attributed to the MIS 21-20 couplet based on its stratigraphic position.

4.2.4. The Marcedusa area

This area was subjected to careful investigation in the badlands that are widely exposed immediately southeast of the Marcedusa village (Fig. 2) and it deserves an in-depth discussion.

5. The petrogallo composite key section

A high-resolution sampling and biostratigraphic analysis based on calcareous nannofossils was performed in this section, both in spot samples and continuous stratigraphic Segments (Fig. 10). Integration of biostratigraphic evidences and extensive field survey unraveled that a swarm of faults and fractures is present in the area, albeit often undetectable in the field given the overall monotonous lithology. No continuous succession could therefore be logged and sampled along a single trajectory. Consequently, our strategy was to focus on well-exposed, undisturbed Segments for attempting the reconstruction of a single composite section.

5.1. The oxygen isotope stratigraphy

The oxygen isotope records of foraminiferal calcite in marine sediments provide a highly resolved standard reference for

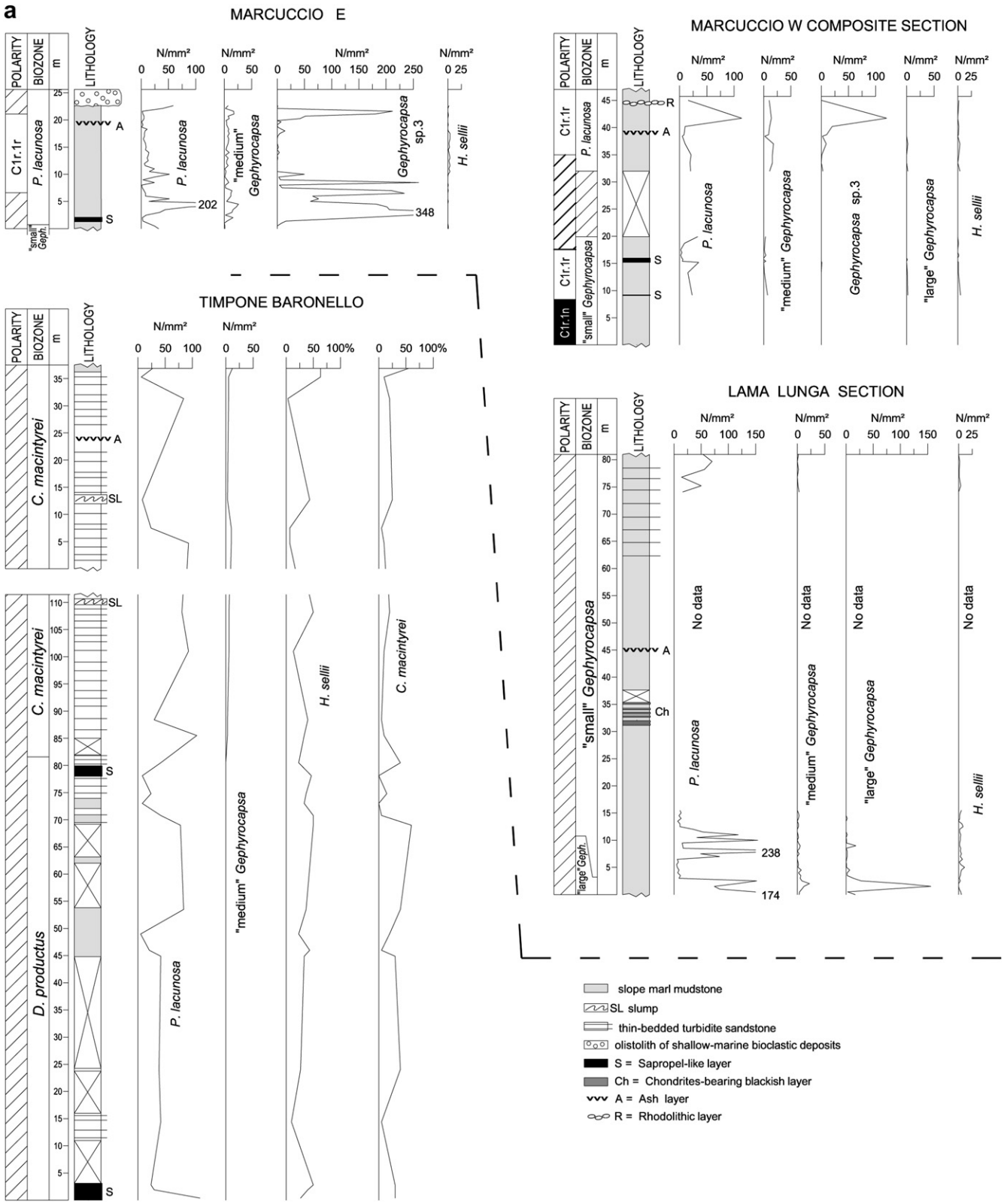

Fig. 5. a, b Details of the logged sections.

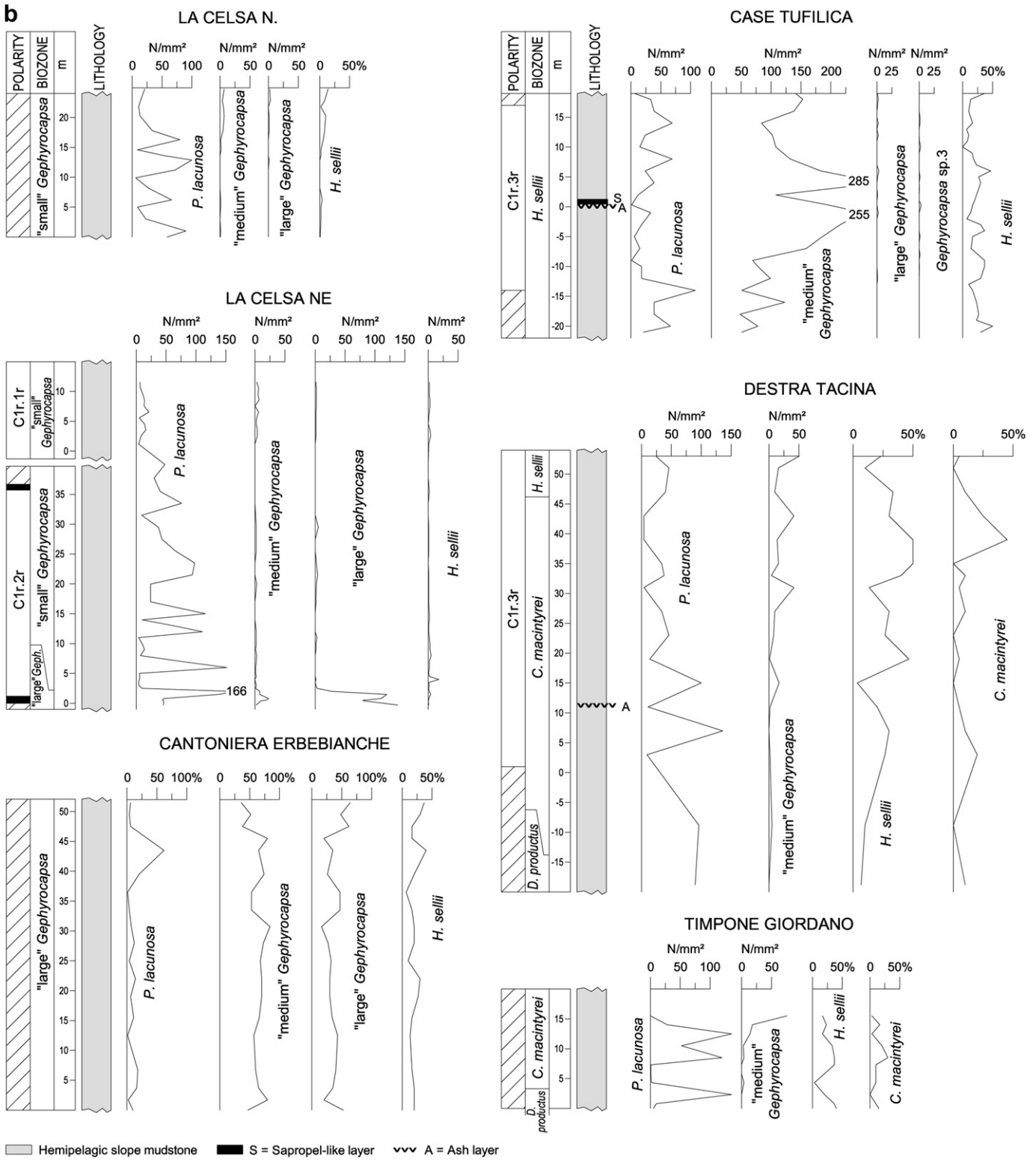

Fig. 5. (*continued*).

Pleistocene chronology and critical paleoenvironmental information, such as eustatic sea level changes (benthic foraminifera) and sea-surface temperature and salinity (planktonic foraminifera). With respect to the open ocean, Mediterranean $\delta^{18}O$ records are generally affected by stronger regional overprints due to local evaporation–precipitation budgets, temperature and circulation (Vergnaud-Grazzini et al., 1977). However, it is suggested that, in spite of the shelfal setting, the oxygen isotope composition of foraminiferal calcite in the Valle di Manche section is primarily controlled by changes in the global ice volume (see Capraro et al., 2005). By comparison, we infer that also the $\delta^{18}O$ variability in the neighboring Petrogallo succession, which was laid in a deeper

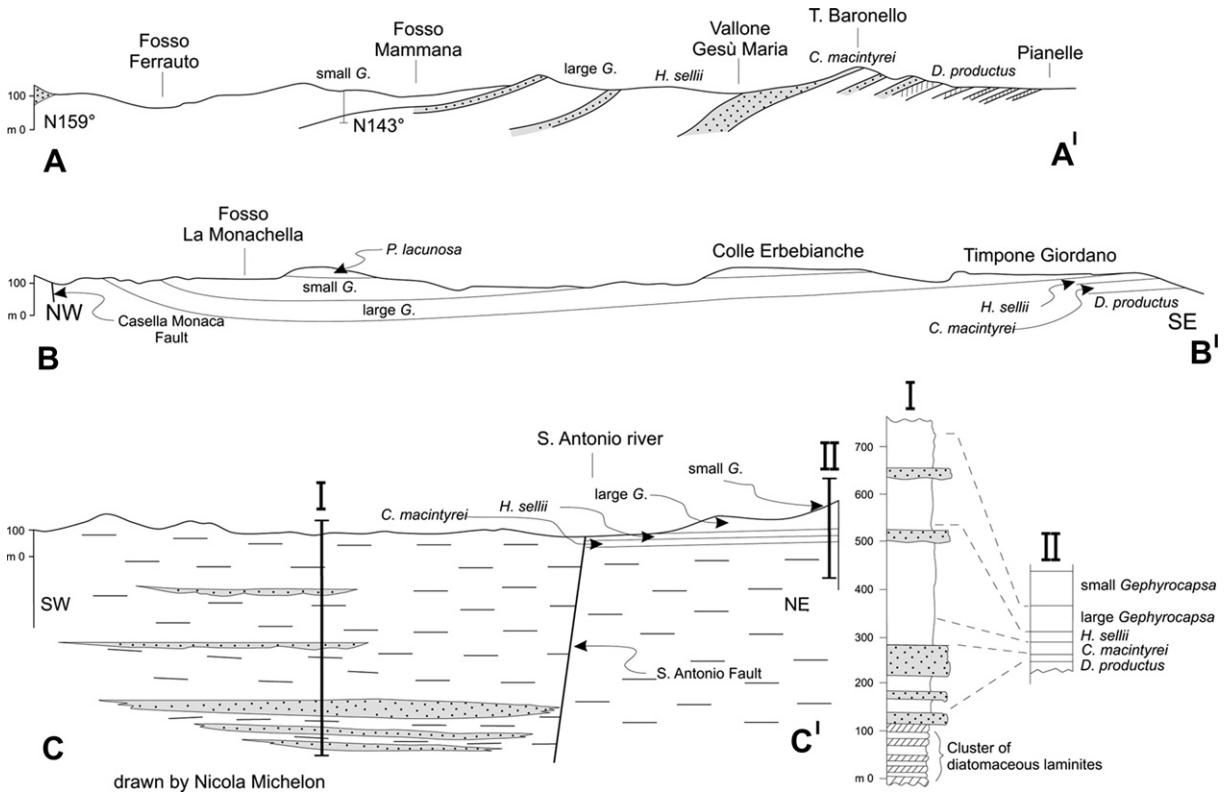

Fig. 6. Contrasting stratigraphic architectures between Sectors 1 and 3 (traces of the sections are in Fig. 3).

setting than the Valle di Manche section, is likely to correlate with the standard global MIS (Fig. 10). Here we restrain from further in-depth discussions that are however available in Capraro et al. (2005). In our record, the $\delta^{18}O_{benthic}$ of *Uvigerina peregrina* varies from ca 4‰–1.5‰ (Fig. 10). The "lightest" values correspond predictably with the finer lithologies (Fig. 10). Being fully comparable with the isotopic composition of modern *Uvigerina* spp. in the eastern Mediterranean (Vergnaud-Grazzini et al., 1986), we interpret values close to 2.0‰, or "lighter", as indicative of full interglacial conditions. Interpretation of glacial intervals is less straightforward: the heaviest values of *U. peregrina* are around 4‰, thus "lighter" than those reported by Vergnaud-Grazzini et al.

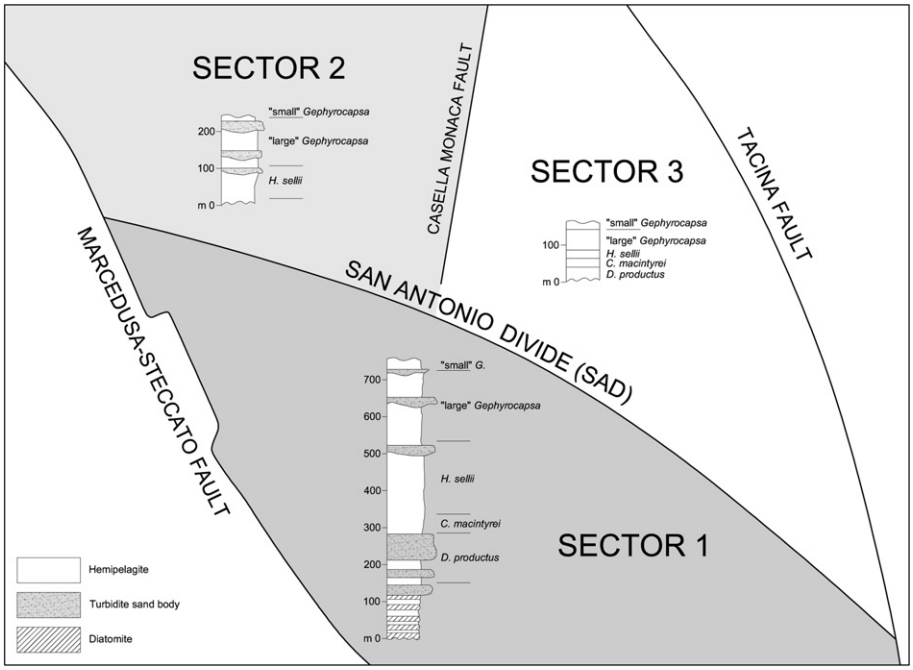

Fig. 7. The three sectors where the Lower Pleistocene succession shows different thickness and internal architecture, and schematic respective stratigraphy.

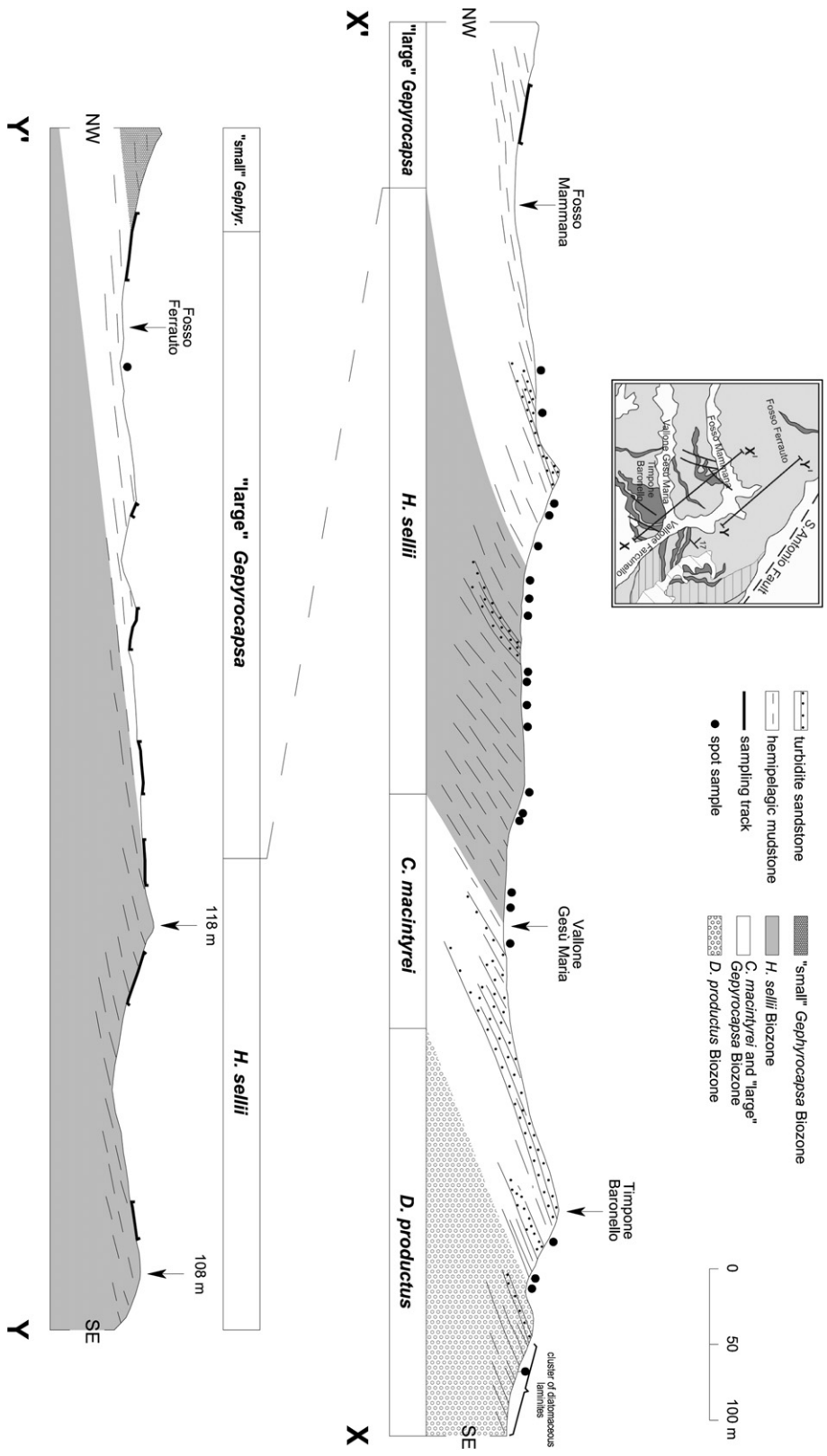

Fig. 8. Sample location and biostratigraphy of the Lower Pleistocene succession across two transects (X–X′ and Y–Y′) in Sector 1 (traces in Fig. 2); the vertical scale equals the horizontal.

(1986) for *Uvigerina* spp. during the last glacial maximum (average of 4.5‰). In addition, the maximum amplitude shown by *U. peregrina* (ca 2.1‰) is larger than that observed in deep-sea sediments (1.5‰: Shackleton and Opdyke, 1973). However, the benthic values in our samples reflect bottom water temperatures on upper slope or outer shelf, and cannot be compared directly to the deep-sea environment. Therefore, in our depositional setting, we consider values of 4‰, or heavier, as indicative of full glacial conditions.

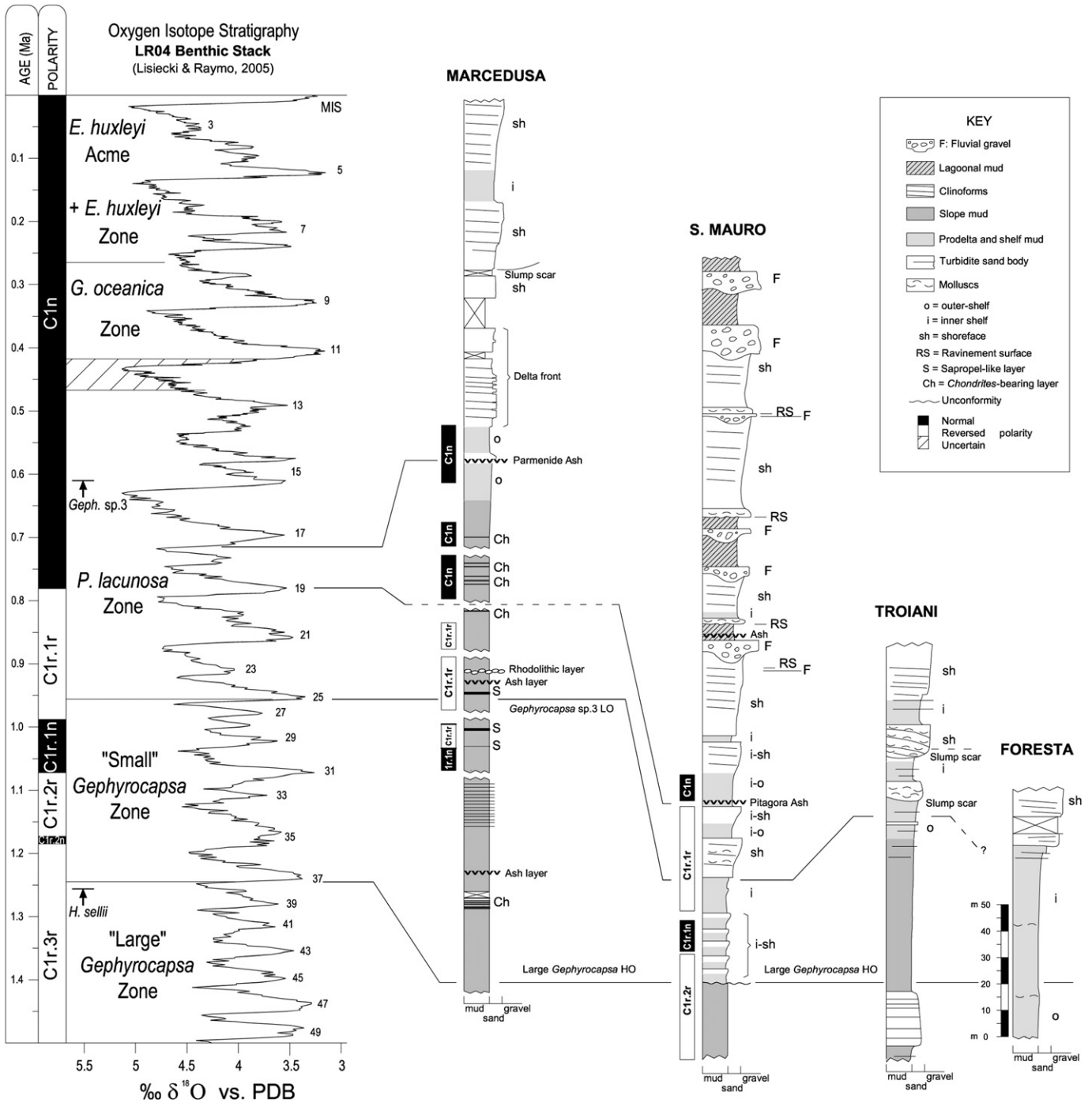

Fig. 9. Stratigraphic correlation in the upper part of the succession.

The variation pattern of $\delta^{18}O_{planktonic}$ for the surface dweller *Globigerinoides ruber,* where available, closely follows that of *U. peregrina* (Fig. 10). The oxygen isotopic composition of recent *G. ruber* in the Mediterranean reflects temperature and salinity gradients, as it displays a decreasing trend from the western (+0.64‰) to the eastern basins (−1.04‰) (Vergnaud-Grazzini et al., 1986). In the Ionian Sea, values are intermediate (−0.83‰) and compare well with the "light" values observed in the Petrogallo section (ca −1‰). In Segments A and E, however, spikes of much "lighter" $\delta^{18}O$ values are found (Fig. 10), suggesting the onset of anomalous conditions in the basin surface waters with respect to the intervening $\delta^{18}O$ interglacials. These anomalies may be explained either in terms of exceptionally high temperature and/or low salinity conditions in the Central Mediterranean surface waters. However, the extremely "light" $\delta^{18}O$ episode (ca −2‰) documented in Segment A (Fig. 10) developed during the deposition of a laminated, sapropel-like layer, thus suggesting a transient emplacement of a very fresh surface water mass, depleted in ^{18}O, in the Central-Eastern Mediterranean (Rohling, 1994) rather than an increase in water temperatures. By comparison, we tentatively interpret the "light" $\delta^{18}O$ values in Segment E as the response to similar oceanographic conditions which, in the case, occurred in

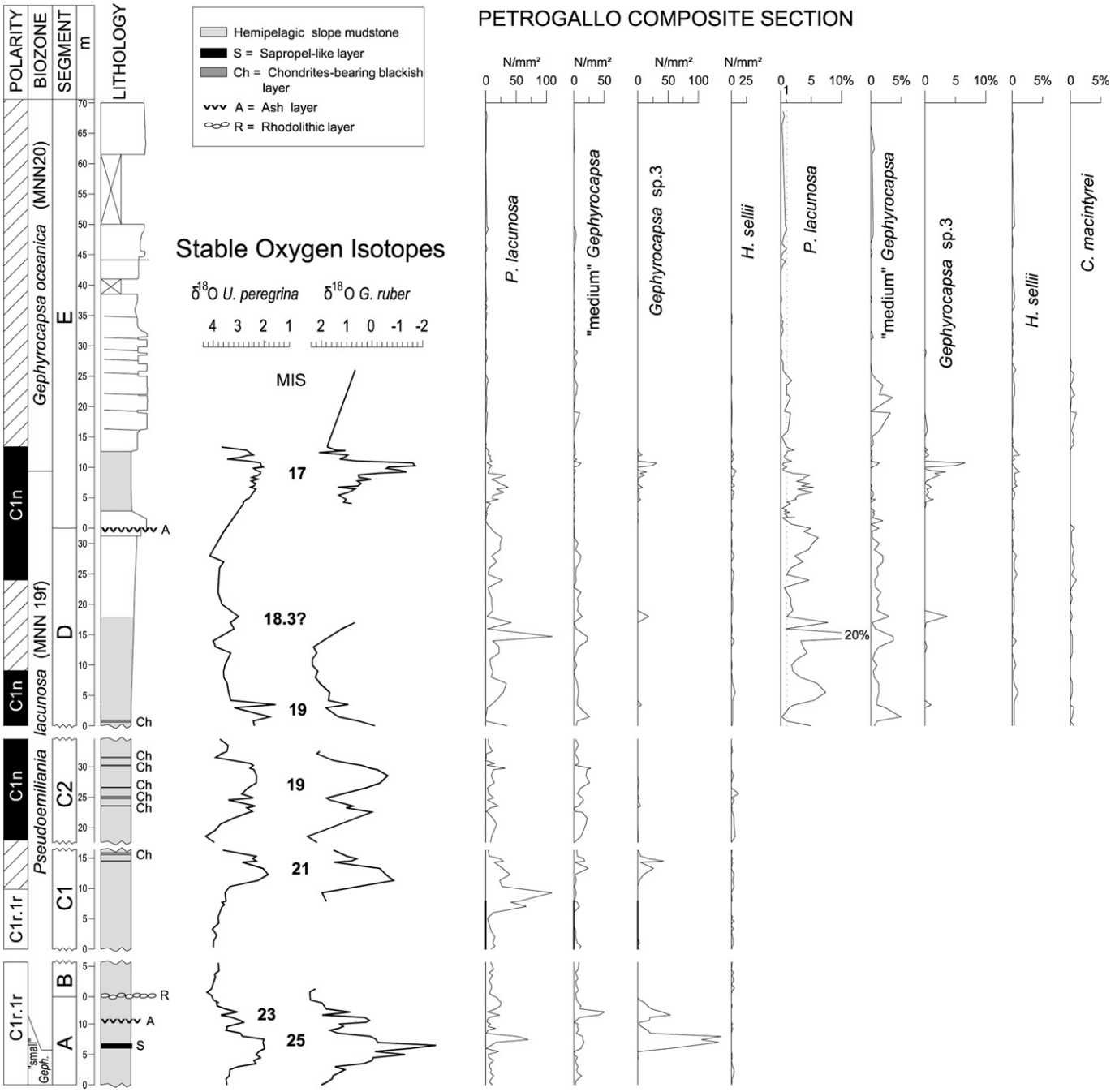

Fig. 10. The composite Petrogallo section.

a shallower-water environment, unsuitable to the deposition/preservation of laminated (sapropel-like) facies.

The heaviest (glacial) values in our record are in excess of +2.0‰, which result in an average glacial–interglacial $\delta^{18}O$ range close to 3‰. As stated above, a direct comparison between $\delta^{18}O_{G.\ ruber}$ records from the Mediterranean is difficult, as this species responds promptly to the vastly different oceanographic conditions in the Basin. However, our values are comparable to the average range of 2.9‰ observed during the last glacial termination in the eastern Mediterranean (Thunell and Williams, 1989) and to what observed in the Ionian Sea core KC01B, where the glacial–interglacial range of *G. ruber* is slightly larger than 3‰ (Langereis et al., 1997; Rossignol-Strick and Paterne, 1999).

5.2. Physical and $\delta^{18}O$ stratigraphy

By means of $\delta^{18}O$ and bio-magneto-stratigraphy, in the basal part of the Petrogallo section (segments A and B in Fig. 10) we achieved evidence of the continuous documentation of the interval from late MIS 26 to MIS 22. Specifically, in Segment A we recognized the LO of *Gephyrocapsa* sp.3 (*sensu* Rio et al., 1990), a distinctive biohorizon that is correlative to MIS 25 in the Mediterranean (Castradori, 1993). In our record, this event occurs close to a laminated, sapropel-like layer, as also emphasized by the very "light" corresponding $\delta^{18}O$ values. Slightly above, a lesser oscillation in the $\delta^{18}O$ record is likely to document with a continuous, albeit condensed, record the MIS 24-MIS 23 glacial-interglacial

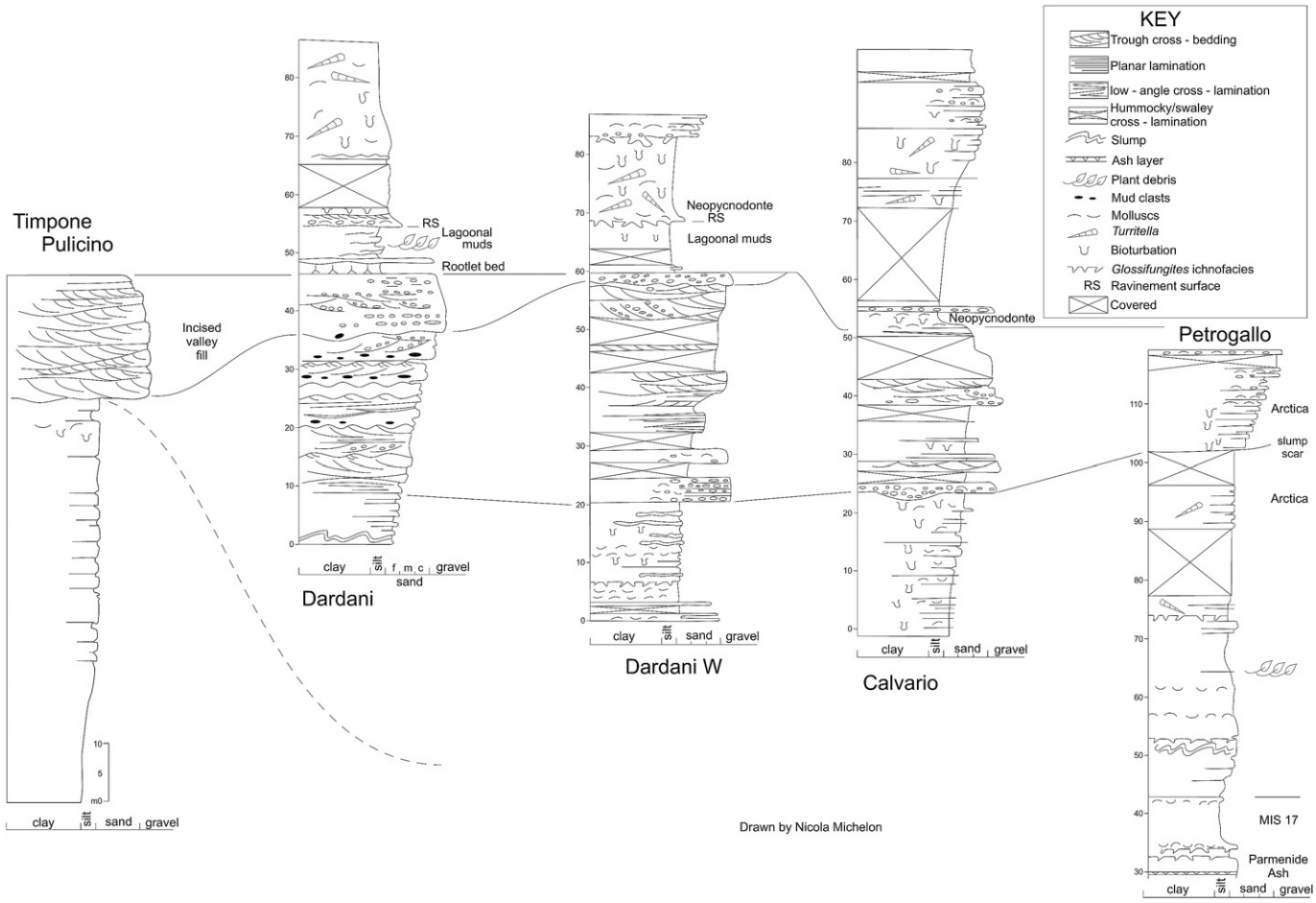

Fig. 11. Correlation between representative sections of the most recent cyclothemic part of the Pleistocene succession within the Marcedusa and Troiani south sub-basins.

cycle. Physical linkage to the overlying Segment B, which is generally dominated by "heavy" $\delta^{18}O$ values, is provided by a unique reddish, bioclastic key layer (up to 9 cm thick), which is underlain (4 m below) by a thin (5–6 cm) ash layer that thickens eastwards. The bioclastic layer consists of rhodoliths, debris of shallow-water molluscs and small quartz and granite pebbles, and can be laterally traced into two large, stratified olistoliths (5.5 and 2.5 m thick) of the same composition. Deposition of this bioclastic layer is interpreted as a dispersal event accompanying the emplacement of olistoliths, which in turn may reflect the collapse of a shelf margin during a lowstand episode. Indeed, $\delta^{18}O$ values from the mudstones embedding the bioclastic layer (Fig. 10) are fully consistent with a severe glacial interval, thus suggesting that its deposition probably took place during the MIS 22 glaciation (Fig. 10). Magnetostratigraphic data support this interpretation, since both Segments A and B are characterized by reversed polarity (Chron C1r). The top of Segment B, i.e., above the prominent bioclastic layer, is characterized by the occurrence of sparse sand layers embedded in a silty matrix.

5.3. The middle-upper part of the Petrogallo section

Chronological interpretation of this part of the record has been exceptionally controversial, and it deserves a special in-depth discussion.

Although a physical linkage is missing, facies similar to those of the underlying Segment B characterize the lower part of Segment C. "Heavy" $\delta^{18}O$ values and inverse polarity component suggest that this part of the stratigraphy was laid during the late MIS 22 glacial. Above, Segment C straddles two full $\delta^{18}O$ interglacials (Fig. 10). They are separated by a distinct $\delta^{18}O$ glacial interval, which could be sampled only partly because of its bad exposure. In Sub-segment C2, all samples show a normal polarity component (Chron C1n). Therefore, this interval lies above the Matuyama-Brunhes magnetic reversal (B/MB) that, so far, was not detected confidently in the Petrogallo badland area. Unfortunately, we could not attain paleomagnetic information for the upper half of Sub-segment C1, which is no longer exposed.

The characters of fine-grained slope sedimentation persist up to the lower part of Segment D, where an upward-shallowing silty package with sparse *Arctica* shells documents a first shift toward shelfal conditions. Segment D was linked to the underlying Segment C by tracing laterally a bundle of distinctive blackish layers. A small overlap exists between Segments C and D, as also indicated by the comparable $\delta^{18}O$ values at the top and bottom of either Segment, respectively (Fig. 10). Segment D encompasses a glacial stage, confined between a late interglacial stage and a glacial termination that occur below and above, respectively (Fig. 10). Peak $\delta^{18}O_{U.\ peregrina}$ events are observed that are in excess of 4‰, namely the "heaviest" $\delta^{18}O$ values of the entire section; however, significant oscillations toward "lighter" $\delta^{18}O$ values occur in both the planktonic and benthic records.

In the uppermost portion of Segment D, a whitish ash layer, 10–15 cm thick, is present (Fig. 10). Based on both its

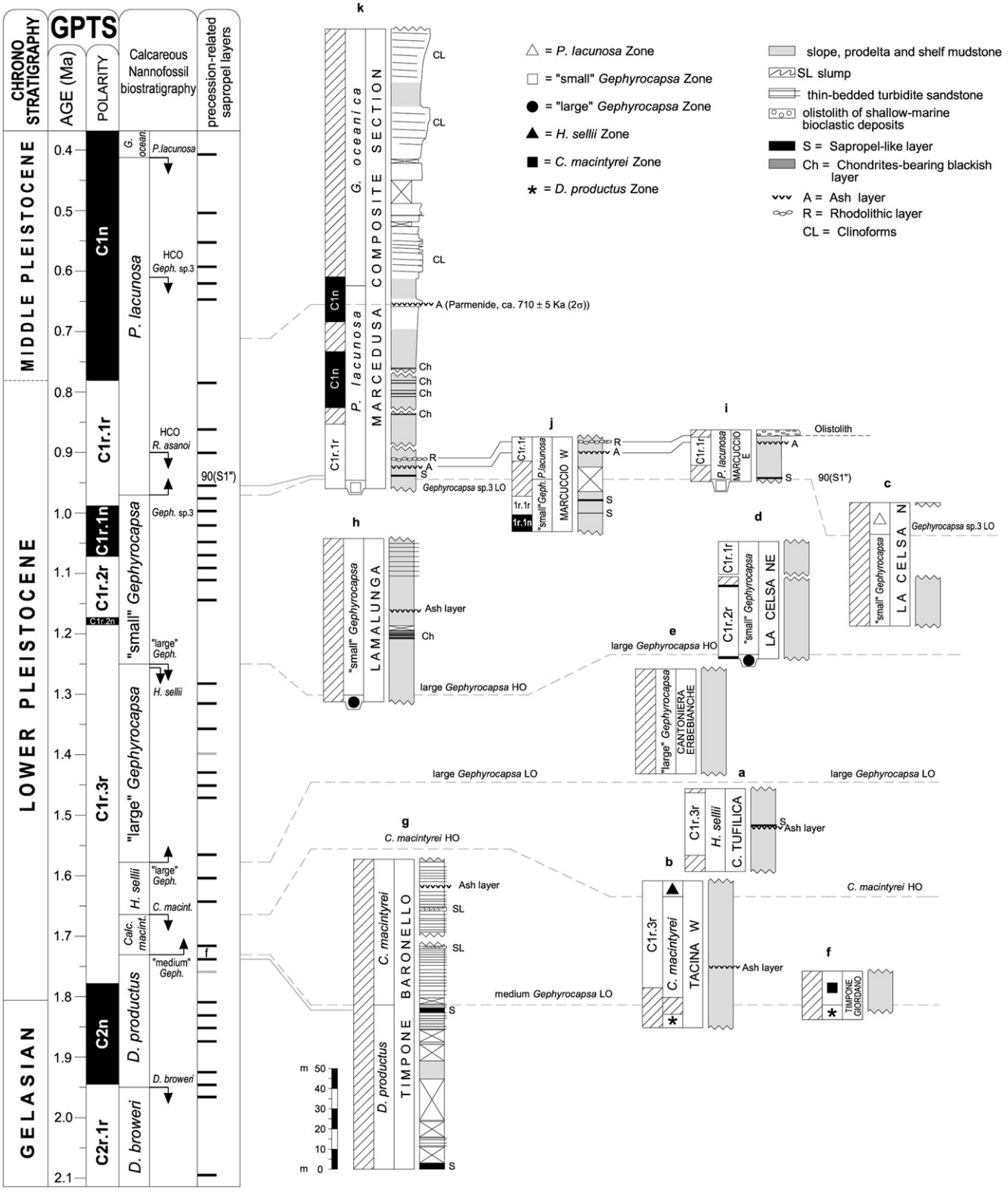

Fig. 12. The reconstructed uppermost Pliocene to upper Middle Pleistocene stratigraphic record in the south-western part of the onshore Crotone Basin. See Fig. 2 for location of sections.

chronostratigraphic position and geochemical characterizations, this ash layer was correlated with the Parmenide ash, first identified in the San Mauro area (Rio et al., 1996; Massari et al., 2002) and labeled accordingly.

Segment E straddles a very prominent interglacial stage, in the midst of which extremely "light" $\delta^{18}O_{G.\ ruber}$ values are observed (Fig. 10). The uppermost part of our $\delta^{18}O$ record (middle Segment E) is represented by a shift toward extreme glacial conditions, albeit

documentation is poor. However, physical stratigraphic evidences indicate a major shallowing with respect to the underlying interglacial, being this part of the succession represented by a ca 60 m thick package of low-angle clinobeds mainly consisting of fine sands and muds with common plant debris and plenty of *Turritella* and *Arctica*, suggesting a distal delta-front facies association linked to a south-easterly prograding delta system.

Chronology of the upper Petrogallo succession was established essentially based on nannofossil biostratigraphy, in the absence of other independent time constraints. Based on the distribution pattern of key species for the Middle Pleistocene interval, two biohorizons were recognized, namely (a) the Highest Occurrence (HO) of *Gephyrocapsa* sp.3 (correlative with MIS 15 in the Mediterranean: Langereis et al., 1997; Castradori, 1993) in the midst of Sub-segment C2, and (b) the HO of *Pseudoemiliania lacunosa*, an event that occurred at the MIS 12-MIS 11 transition in the Mediterranean (Thierstein et al., 1977), in the lower part of Segment E (Fig. 10). Hence, Segments C and D (Fig. 10) were interpreted to document the interval from MIS 15 to MIS 12 and, accordingly, Segment E (Fig. 10) was likely to span from early MIS 11 to full MIS 10 (e.g., Massari et al., 2001). In opposition to this age model, however, was the occurrence of a short-lived, albeit prominent, spike of *Gephyrocapsa* sp. 3 in the midst of the prominent $\delta^{18}O$ interglacial of Segment E (Fig. 10). This evidence was of minor concern nevertheless, as it could be explained either by the input of reworked material from the surroundings or by a transient incursion in the central Mediterranean of this species, presently dwelling in oceanic surface waters off-shore the Strait of Gibraltar (Bukry, 1978; Maiorano and Marino, 2004), in response to anomalous oceanographic and/or climatic conditions.

Geochronological data were retrieved recently from the "Parmenide" ashbed of Petrogallo, which provided an independent key constraint for reconstructing the chronology of the succession. Specifically, 33 Ar/Ar analyses performed on sanidines extracted from the ashbed using procedures as described in Scaillet et al. (2008) indicate, for the Parmenide ash, an age of ca 710 $\pm$ 5 ka (2 s; Scaillet, pers. comm.). The latter is remarkably distant from what inferred previously (i.e., ca 410 ka) based on biostratigraphic evidences. Geochronological analyses are still in progress, and the matter will be discussed widely in a forthcoming, dedicated paper.

When compared to the standard $\delta^{18}O$ records, the age of ca 710 ka estimated for the "Parmenide" ashbed corresponds to the beginning of the MIS 18-MIS 17 transition (Lisiecki and Raymo, 2005), which is in perfect agreement with the stratigraphic position of the "Parmenide" ash in the Petrogallo composite section (i.e., beginning of a glacial termination: Fig. 10). Based on this indication, we developed a new age model for the Petrogallo stratigraphy, according to which Segment C encompasses the MIS 21-MIS 19 interval, Segment D spans from late MIS 19 to early MIS 17 and Segment E covers the MIS 17-MIS 16 interval (Fig. 10). On the whole, this age model is in keeping with the biostratigraphic and magnetostratigraphic evidences. It is also provided that a good documentation of the B/MB is still missing in the Petrogallo badland area, as our correlative MIS 19 (Sub-segment C2; Fig. 10) is characterized entirely by a normal polarity component.

5.4. The younger part of the succession in the Marcedusa area

The deltaic interval attributed to MIS 16 in the Petrogallo section (see above) can be traced proximally, i.e., in the NNW direction, into inferred delta-front amalgamated sands that are abruptly overlain by shallow-water deposits, best exposed in most proximal settings (sections Dardani, Calvario, Dardani W: Fig. 11). The uppermost part of the succession in the Marcedusa area consists of a transgressive–regressive cyclothem up to 50 m thick (Fig. 11). Firm chronological ties for this complex are obviously lacking, and uncertainty is increased by the presence of unconformities and by the unknown rank and character (allocyclic vs. autocyclic) of the sequences.

It deserves to be stressed that, although shallow-marine deposits in the Marcedusa sector show facies and organization similar to those occurring in the San Mauro, Foresta and Troiani areas, they appeared remarkably later in the former (MIS 16) than in the latter, where they begun to be laid down since MIS 24/22 times (Fig. 9).

6. Sedimentation and tectonics

Based on the constraints achieved from the logged sections, a synthetic chronological framework can be attained. Specifically, the uppermost Pliocene to upper Middle Pleistocene interval has been documented almost entirely, albeit not continuously (Fig. 12). This record provides significant clues to the reconstruction of the stratigraphic and geologic evolution of this sector of the Crotone Basin during thePleistocene, which can be subdivided into two main stages: the first is characterized by the activity of the SAD, the second is marked by the apparent confinement of deposition within a number of areas, chiefly bounded by NE to NNE-trending normal faults.

A spectacular effect of Early Pleistocene tectonics is represented by the large difference in stratigraphic architectures between Sectors 1 and 3, on either sides of the SAD, in response to dramatically different subsidence rates (Figs. 6 and 7). We cannot provide a precise age of the onset of regional uplift. Nevertheless, data discussed in this paper provide a sound background for evaluating the history of recent uplift in the Crotone area.

7. Conclusions

Biostratigraphic data based on calcareous nannofossils, integrated by magnetostratigraphic data, document that in the onshore Crotone Basin a large part of the Lower and Middle Pleistocene is represented. Depositional rates are affected by large non-linear variations, suggesting that changes in sediment supply and ultimately the stratigraphical architecture are driven by complex relationships between regional tectonics, eustasy and orbitally-forced climate changes. In addition, synsedimentary faulting resulted in a compartmentalization of the area into separate blocks experiencing differential vertical movements. By integrating biostratigraphic evidences and physical stratigraphy, we demonstrate that major structural divides (the SAD in particular) fully controlled sedimentation rates and styles during the earlier Pleistocene, with dramatic differences in the thickness of the stratigraphic successions on very short distances. Afterward, higher subsidence rates are likely to have affected the Marcedusa area, where the appearance of shallow-water facies dates to MIS 16 times, ca 300 kyr later than in the surrounding areas (namely Troiani, Foresta and San Mauro).

For the upper Lower Pleistocene and Middle Pleistocene part of the succession, a detailed oxygen isotope stratigraphy was established in the Petrogallo section, which revealed a repetition of glacial–interglacial stages apparently in agreement with the standard $\delta^{18}O$ reference records, and, by integration with bio-magnetostratigraphic data, provided a high-resolution chronologic framework possibly up to MIS 17.

Firm chronological tie points in the uppermost part of the succession, where sedimentation becomes shallow-marine to continental, are missing. Albeit a precise age of the onset of regional uplift cannot be pinned, our data are likely to provide a firm constraint for assessing the timing and rates of recent uplift in the study area.

Acknowledgments

Special thanks go to the anonymous Reviewers for their thoughtful contribution and helpful criticism. We are indebted to the Editorial Staff of Quaternary Science Reviews and particularly to Dr José S. Carrion, Co-Editor, for their help and indulgence. Technical support was provided by Nicola Michelon and Alessandra Asioli. This work was funded by MIUR (PRIN 2006 to F. Massari).

References

Anderson, H., Jackson, J., 1987. The deep seismicity of the Tyrrhenian Sea. Geophys. J. Roy. Astr. Soc. 91, 613–637.

Backman, J., Shackleton, N.J., 1983. Quantitative biochronology of Pliocene and early Pleistocene nannofossils from the Atlantic, Indian and Pacific oceans. Mar. Micropaleontol. 8, 141–1770.

Barone, A., Fabbri, A., Rossi, S., Sartori, R., 1982. Geological structure and evolution of the marine areas adjacent to the Calabrian Arc. Earth Evol. Sci. 3, 207–221.

Bukry, D., 1978. Cenozoic coccolith and silicoflagellate stratigraphy, offshore northwest Africa, deep Sea drilling project leg 41. In: Lancelot, Y., Seibold, E., et al. (Eds.), DSDP. Init. Rep. 41, 689–707.

Capraro, L., Asioli, A., Backman, J., Bertoldi, R., Channell, J.E.T., Massari, F., Rio, D., 2005. Climatic patterns revealed by pollen and oxygen isotope records across Brunhes-Matuyama boundary in the central Mediterranean (Southern Italy). In: Head, M.J., Gibbard, P.L. (Eds.), Geol. Soc. Spec. Publ, vol. 247, pp. 159–182.

Carobene, L., Dai Pra, G., 1990. Genesis, chronology and tectonics of the Quaternary marine terraces of the Tyrrhenian coast of Northern Calabria (Italy). Their correlation with climatic variations. Il Quaternario 3, 75–94.

Castradori, D., 1993. Calcareous nannofossil biostratigraphy and biochronology in eastern Mediterranean deep-sea cores. Riv. It. Pal. Strat 99, 107–126.

Van Dijk, J.P., 1992. Late Neogene fore-arc basin evolution in the Calabrian Arc (central Mediterranean); tectonic sequence stratigraphy and dynamic geohistory. With special reference to the geology of Central Calabria. Geol. Ultraiect. 92, 288.

Goes, S., Giardini, D., Jenny, S., Hollenstein, C., Kahle, H.G., Geiger, A., 2004. A recent tectonic reorganization in the south-central Mediterranean. Earth Planet. Sci. Lett. 226, 335–345.

Istituto Nazionale di Geofisica e Vulcanologia, 2007. Italian magnetic network and geomagnetic field maps of Italy at year 2005. Bollettino di Geodesia e Scienze affini Anno LXVI, 1.

Jenny, S., Goes, S., Giardini, D., Kahle, H.G., 2006. Seismic potential of southern Italy. Tectonophysics 415, 81–101.

Kirschvink, J.L., 1980. The least-square line and plane and the analysis of paleomagnetic data. Geophys. J. Roy. Astr. Soc. 62, 699–718.

Langereis, C.G., Dekkers, M.J., de Lange, G.J., Paterne, M., van Santvoort, P.J.M., 1997. Magnetostratigraphy and astronomical calibration of the last 1.1 Myr from an eastern Mediterranean piston core and dating of short events in the Brunhes. Geophys. J. Int. 129, 75–94.

Lanzafame, G., Tortorici, L., 1981. La tettonica recente della valle del fiume Crati (Calabria). Geografia Fisica e Dinamica Quaternaria 4, 11–21.

Lisiecki, L.E., Raymo, M.E., 2005. A Plio-Pleistocene stack of 57 globally distributed benthic $\delta^{18}O$ records. Paleoceanography 20, PA1003. doi:10.1029/2004PA001071.

Lourens, L.J., 2004. Revised tuning of ocean drilling program Site 964 and KC01B (Mediterranean) and implications for the $\delta^{18}O$, tephra, calcareous nannofossil, and geomagnetic reversal chronologies of the past 1.1 Myr. Paleoceanography 19, PA3010. doi:10.1029/2003PA000997.

Lourens, L.J., Antonarakou, A., Hilgen, F.J., Van Hoof, A.A.M., Vergnaud-Grazzini, C., Zachariasse, W.J., 1996. Evaluation of the Plio-Pleistocene astronomical timescale. Paleoceanography 11, 391–413.

Lucente, F.P., Chiarabba, C., Cimini, G.B., Giardini, D., 1999. Tomographic constraints on the geodynamic evolution of the Italian region. J. Geophys. Res. 104, 307–327.

Maiorano, P., Marino, M., 2004. Calcareous nannofossil bioevents and environmental control on temporal and spatial patterns at the Early–Middle Pleistocene. Mar. Micropaleontol. 53, 405–422.

Malinverno, A., Ryan, W.B.F., 1986. Extension on the Tyrrhenian Sea and shortening in the Apennines as result of arc migration driven by sinking of the lithosphere. Tectonics 5, 227–245.

Massari, F., Sgavetti, M., Rio, D., D'Alessandro, A., Prosser, G., 1999. Composite sedimentary record of falling stages of Pleistocene glacio-eustatic cycles in a shelf setting (Crotone Basin, south Italy). Sediment. Geol. 127, 85–110.

Massari, F., Rio, D., Sgavetti, M., Asioli, A., Backman, J., Capraro, L., D'Alessandro, A., Fornaciari, E., Prosser, G., 2001. The middle Pleistocene of the Crotone Basin. In: Ciaranfi, N., Pasini, G., Rio, D. (Eds.), The Meeting on the Plio-Pleistocene Boundary and the Lower/Middle Pleistocene Transition: Type Areas and Sections. Mem. Sci. Geol. 53, 85–112 (Bari, 25–29 September 2000).

Massari, F., Rio, D., Sgavetti, M., Prosser, G., D'Alessandro, A., Asioli, A., Capraro, L., Fornaciari, E., Tateo, F., 2002. Interplay between tectonics and glacio-eustasy: Pleistocene succession of the Crotone Basin, Calabria (southern Italy). Geol. Soc. Am. Bull. 114, 1183–1209.

Massari, F., Capraro, L., Rio, D., 2007. Climatic modulation of timing of systems-tract development with respect to sea-level changes (middle Pleistocene of Crotone, Calabria, Southern Italy). J. Sediment. Res. 77, 461–468.

Mauz, B., Hassler, U., 2000. Luminescence chronology of Late Pleistocene raised beaches in southern Italy: new data of relative sea-level changes. Mar. Geol. 170, 187–203.

Molin, P., Pazzaglia, F.J., Dramis, F., 2004. Geomorphic expression of active tectonics in a rapidly-deforming forearc, Sila massif, Calabria, southern Italy. Am. J. Sci. 304, 559–589.

Nalin, R., Lamothe, M., Auclair, M., Massari, F., 2007. Using Optically Stimulated Luminescence (OSL) to Unravel the Chronology and Deformation History of Marine Terraces: An Example from the Crotone Peninsula (Southern Italy). In: Geoitalia, Spoleto 2005, Epitome 1, p. 172.

Ogniben, L., 1955. Le argille scagliose del Crotonese. Mem. Note Ist. Geol. Appl. Napoli 6, 1–72.

Patacca, E., Scandone, P., 2004. The Plio-Pleistocene thrust belt-foredeep system in the southern Apennines and Sicily (Italy). In: Crescenti, U., D'Offizi, S., Merlino, S., Sacchi, L. (Eds.), Geology of Italy. Spec. Vol. It. Geol. Soc. IGC 32 Florence-2004, pp. 93–129.

Patacca, E., Sartori, R., Scandone, P., 1993. Tyrrhenian basin and Apennines. Kinematic evolution and related dynamic constraints. In: Boschi, E., et al. (Eds.), Recent Evolution and Seismicity of the Mediterranean Region. Kluwer Acad. Publ, pp. 161–171.

Raffi, I., Backman, J., Rio, D., Shackleton, N., 1993. Plio-Pleistocene nannofossil biostratigraphy and calibration to oxygen isotope stratigraphies from deep sea drilling project Site 607 and ocean drilling program site 677. Paleoceanography 8, 387–408.

Raffi, I., Backman, J., Fornaciari, E., Pälike, H., Rio, D., Lourens, L., Hilgen, F., 2006. A review of calcareous nannofossil astrobiochronology encompassing the past 25 million years. Quat. Sci. Rev. 25, 3113–3137. CITATA IN QUALCHE FIGURA DI SCHEMA CRONOLOGICO?? Se no è da togliere.

Rio, D., Raffi, I., Villa, G., 1990. Pliocene–Pleistocene calcareous nannofossil distribution patterns in the western Mediterranean. In: Kastens, K.A., Mascle, J., et al. (Eds.), Proc. ODP Sci. Res, vol. 107, pp. 513–533.

Rio, D., Channell, J.E.T., Massari, F., Poli, M.S., Sgavetti, M., D'Alessandro, A., Prosser, G., 1996. Reading Pleistocene eustasy in a tectonically active siliciclastic shelf setting (Crotone peninsula, southern Italy). Geology 24, 743–746.

Ritsema, A.R., 1979. Active or passive subduction at the Calabrian Arc. In: Van der Linden, W.J.M. (Ed.), Fixism, Mobilism or Relativism: Van Bemmelen's Search for Harmony. Geol. Mijnbouw 58, 127–134.

Roda, C., 1964. Distribuzione e facies dei sedimenti Neogenici del Bacino Crotonese. Geol. Rom. 3, 319–366.

Rohling, E.J., 1994. Review and new aspects concerning the formation of eastern Mediterranean sapropels. Mar. Geol. 122, 1–28.

Rossi, S., Sartori, R., 1981. A seismic reflection study of the External Calabrian arc in the northern Ionian Sea (eastern Mediterranean). Mar. Geophys. Res. 4, 403–426.

Rossignol-Strick, M., Paterne, M., 1999. A synthetic pollen record of the eastern Mediterranean sapropels of the last 1 Ma: implications for the time-scale and formation of sapropels. Mar. Geol. 153, 221–237.

Sartori, R., 1990. The main results of ODP Leg 107 in the frame of Neogene to recent geology of perityrrhenian areas. In: Kastens, K.A., Mascle, J., et al. (Eds.), Proc. ODP Sci. Res, vol. 107, pp. 715–730.

Sartori, R., 2003. The Tyrrhenian back-arc basin and subduction of the Ionian lithosphere. Episodes 26, 217–221.

Scaillet, S., Vita-Scaillet, G., Guillou, H., 2008. Oldest human footprints dated by Ar/Ar. Earth Planet. Sci. Lett. 275, 320–325.

Schiattarella, M., Di Leo, P., Benedice, P., Giano, S.I., Martino, C., 2006. Tectonically driver exhumation of a young orogen: an example from the southern Apennines, Italy. In: Willett, S.D., Hovius, N., Brandon, M.T., Fisher, D.M. (Eds.), Tectonics, Climate, and Landscape Evolution. Geol. Soc. Am. Spec. Paper 398, Penrose Conf. Series, pp. 371–385.

Shackleton, N.J., Opdyke, N.D., 1973. Oxygen isotope and paleomagnetic stratigraphy of equatorial Pacific core V28-289: oxygen isotope temperatures and ice volumes on a 105-year and 106-year scale. Quaternary Res. 3, 39–55.

Thierstein, H.R., Geitzenauer, K.R., Molfino, B., Shackleton, N.J., 1977. Global synchronicity of late Quaternary coccolith datum levels: validation by oxygen isotopes. Geology 5, 400–404.

Thunell, R.C., Williams, D.F., 1989. Glacial–Holocene salinity changes in the Mediterranean Sea: hydrographic and depositional effects. Nature 338, 493–496.

Tortorici, L., Monaco, C., Tansi, C., Cocina, O., 1995. Recent and active tectonics in the Calabrian arc (Southern Italy). Tectonophysics 243, 37–55.

Van Dijk, J.P., 1991. Basin dynamics and sequence stratigraphy in the Calabrian arc (Central Mediterranean); records and pathways of the Crotone Basin. Geol. Mijnbouw 70, 187–201.

Van Dijk, J.P., Okkes, M., 1991. Neogene tectonostratigraphy and kinematics of Calabrian basins; implications for the geodynamics of the Central Mediterranean. Tectonophysics 196, 23–60.

Vergnaud-Grazzini, C., Ryan, W.B.F., Cita, M.B., 1977. Stable isotopic fractionation, climate change and episodic stagnation in the eastern Mediterranean during the late Quaternary. Mar. Micropaleontol. 2, 353–370.

Vergnaud-Grazzini, C., Glacon, G., Pierre, C., Pujol, C., Urrutiaguer, M.J., 1986. Foraminifères planctoniques de Méditerranée en fin d'été. Relations avec les structures hydrologiques. Mem. Soc. Geol. It 36, 175–188.

Westaway, R., 1993. Quaternary uplift of southern Italy. J. Geophys. Res. 98, 21741–21772.

Zijderveld, J.D.A., 1967. AC demagnetization of rocks: analysis of results. In: Runcorn, S.K., Creer, K.M., Collinson, D.W. (Eds.), Methods in Palaeomagnetism. Elsevier, Amsterdam, pp. 254–286.